Microstructural evolution during austempering of a ASTM A-532 CLASS III type high chromium white cast iron undergoing abrasive wear

Evolución microestrutural durante austemperado de una fundición blanca al alto cromo ASTM A-532, Clase III, Tipo A, sometida a desgaste abrasivo

Evolução microestrutural durante austemperado de uma fundição branca ao alto cromo ASTM A-532, Classe III, Tipo A, submetida a desgaste abrasivo

Oscar Fabián Higuera-Cobos*
Jeison Bucurú-Vasco**
Andrés Felipe Loaiza-Patiño***
Mónica Johanna Monsalve-Arias****
Dairo Hernán Mesa-Grajales*****

Fecha de recepción: 23 de julio de 2017
Fecha de aceptación: 17 de agosto de 2017

Abstract

This paper studies the influence of variables such as holding temperatures and times during austempering of High Chromium White Cast Iron (HCWCI), with the following chemical composition: Cr 25 %, C 3 %, Si 0.47 %, Mn 0.74 % and Mo 1.02 %. The aim of the austempering was to modify the percentage of retained austenite and its correlation to abrasive wear resistance under different conditions. Microhardness tests, SEM-EDS and XRD were performed to determine mechanical properties, chemical composition, and type of carbides and microstructures present, respectively. The tests complied with the ASTM G-65 standard. Results showed that the best performance against abrasion was achieved for austempering at 450 ºC with holding time of 6 hours.

Keywords: Austempered; Retained austenite; Abrasive wear; High chromium white cast iron; Chromium carbides.

Resumen

Este trabajo estudia la influencia de variables tales como *tiempo* y *temperatura de sostenimiento* durante el austemperado de una fundición blanca al alto cromo con la siguiente composición: Cr, 25 %; C, 3 %; Si, 0.47 %; Mn, 0.74 %, y Mo, 1.02 %. El objetivo del austemperado fue modificar el porcentaje de austenita retenida, y

* Ph. D. Universidad del Atlántico (Barranquilla-Atlántico, Colombia). oscarhiguera@mail.uniatlantico.edu.co. ORCID: 0000-0002-4836-5215.
** Universidad Tecnológica de Pereira (Pereira-Risaralda, Colombia).
*** Universidad Tecnológica de Pereira (Pereira-Risaralda, Colombia).
**** Ph. D. Universidad del Atlántico (Barranquilla-Atlántico, Colombia). monicamonsalve@mail.uniatlantico.edu.co. ORCID: 0000-0002-9902-8518.
***** Ph. D. Universidad Tecnológica de Pereira (Pereira-Risaralda, Colombia). dhmesa@utp.edu.co.

correlacionarlo con la resistencia al desgaste abrasivo bajo diferentes condiciones; los ensayos fueron realizados según los lineamientos de la norma ASTM G65. Las técnicas de microdureza MEB-EDS y DRX fueron realizadas para determinar las propiedades mecánicas, composición química, tipo de carburos y microestructuras presentes, respectivamente. Los resultados mostraron que la mejor resistencia a la abrasión fue alcanzada a una temperatura de austemperado de 450 ºC y a 6 horas de permanencia.

Palabras clave: Austemperado; Austenita retenida; Desgaste abrasivo; Fundiciones al alto cromo; Carburos de cromo.

Resumo

Este trabalho estuda a influência de variáveis tais como *tempo* e *temperatura de sustentabilidade* durante o austemperado de uma fundição branca ao alto cromo com a seguinte composição: Cr, 25 %; C, 3 %; Si, 0.47 %; Mn, 0.74 %, e Mo, 1.02 %. O objetivo do austemperado foi modificar a porcentagem de austenita retida, e correlacioná-lo com a resistência ao desgaste abrasivo sob diferentes condições; os ensaios foram realizados segundo as diretrizes da norma ASTM G65. As técnicas de microdureza MEB-EDS e DRX foram realizadas para determinar as propriedades mecânicas, composição química, tipo de carbonetos e microestruturas presentes, respectivamente. Os resultados mostraram que a melhor resistência à abrasão foi alcançada a uma temperatura de austemperado de 450 ºC e a 6 horas de permanência.

Palavras chave: Austemperado; Austenita retida; Desgaste abrasivo; Fundições ao alto cromo; Carbonetos de cromo.

I. Introduction

White cast irons are ferrous alloys whose main constituents are chromium and carbon. They have hypoeutectic and hypereutectic compositions consisting in a hard carbide phase ($M_{23}C_6$, M_7C_3 and M_3C) in a hardening matrix. These alloys are commonly used, mostly in the mining sector, mineral grinding and processing, and slurry pumps in the cement industries. Particularly, HCWCI has become a highly demanded material, due to its high hardness, abrasion and oxidation/corrosion resistance. HCWCI may have either a martensitic or austenitic microstructure with a high content of eutectic carbides. M_7C_3 eutectic carbide has a hexagonal crystalline structure with hardness ranging from 1200 to 1800 HV. Usually, austenizing temperatures of white cast iron range from 800 to 1100 °C [1]. Besides the selected temperature, holding time and quenching severity also influence the type of microstructure and second phase particles. Hardness depends on both the amount of precipitate of secondary fine carbides and the transformation from austenite to martensite [2]. In most cases, the material undergoes quenching to obtain a martensite matrix with little amount of retained austenite and precipitate carbides. This heterogeneous structure provides a material with high wear resistance and significant toughness [3].

Since most high chromium cast applications require high abrasive wear resistance, test must be run to guarantee the selection of the best material. Nonetheless, the values of wear resistance can fluctuate considerably, depending on combinations and properties of constituents, and also on test parameters such as load and abrasive agent size. Hence, it is necessary to standardize the tests, otherwise performance classifications must be established based on particular results [3]. HCWCI abrasive resistance can be modified by adjusting proportions, shapes and types of carbides. Likewise, relative hardness and matrix toughness can be determinant factors. Required properties are obtained with cautious control over material composition, procedure path and final heat treatment [4].

II. Experimental procedure

A. Material characterization

In this study, we used HCWCI manufactured by a local company; the material was subsequently subjected to metallographic analysis and characterization by means of optical emission spectrometry using a ARL ASSURE spectrometer, SEM-EDS with a JEOL JSM 5910 electronic microscope, and XRD using a Phillips X´pert Pro Panalytical diffractometer equipped with a RX generator and an empyrean tube (Cu Kα, λ= 1.5406 Å). Table 1 summarizes the chemical composition of the material. Based on values reported for the major constituents (C and Cr), the material can be classified as Class III, type A, in accordance with the ASTM A532 standard [5].

Table 1
HCWCI Chemical Composition

Element	C	Si	Mn	Mo	Fe	Cr	P	S
wt. %	3.02	0.47	0.74	1.02	69.69	24.93	0.126	0.003

B. Heat treatments

All samples were destabilized at 950 ºC for 1 hour, then they were temporarily removed from the furnace until their temperatures nearly decreased to the pre-established values of austempering treatment (650, 450, 350, 250 and 150 °C), then, the samples were taken back to furnace, thereby achieving the completion of the isothermal treatment. Austempering holding times for each pre-established temperature were estimated with the assistance of the isothermal transformation diagram (Fig. 1), and were verified by equations (1), (2) and (3) that model transient heat transfer [6].

$$T = (T_i\text{-}T_\infty)e^{\frac{-Bit}{l^2}} \quad (1)$$

$$Bi = \frac{hl}{k} \quad (2)$$

$$l = \frac{Specimen\ volume}{Contacting\ surface\ submerged\ in\ fluid} \quad (3)$$

Where T and T_∞ denote the austempering temperature and the room temperature respectively; T_i expresses the sample temperature when is removed from the furnace after austenizing. Additionally, the convective heat transfer coefficient, the thermal conductivity of the material, and the time the sample takes to reach T_i are given by *h, k* and *t,* respectively. Estimated *t* values are shown in Table 2. Fig. 1 shows that the transformation final time is about 12 hours for the working temperature interval. For each isothermal treatment, whose *t* (initial austempering time) is indicated in Table 2, specimens were austempered during the following holding times: 3, 6, 9 and 12 hours. Finally, all samples underwent water quenching.

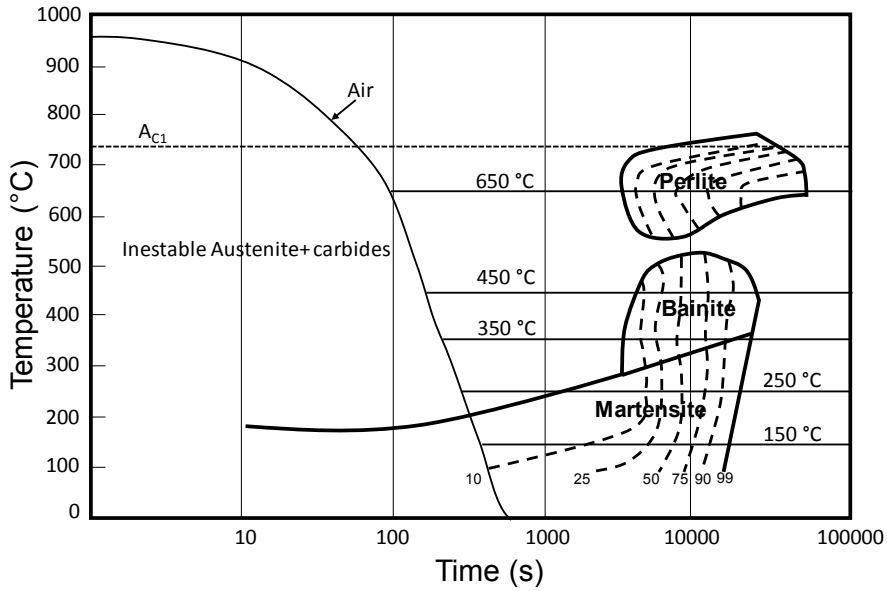

Fig. 1. Conditions for isothermal transformation of white cast iron ASTM A532 Class III Type A [7].

Table 2

Initial times of isothermal treatments for each austempering temperature

Temperature (°C)	950	650	450	350	250	150
Time (s)	0.00	105.6	209.4	282	381.6	540

C. Tests of abrasive wear resistance

Three-body abrasive wear testing was carried out with a dry sand/rubber wheel apparatus (Fig. 2), following the procedure A from the ASTM G65 standard. The following test parameters were used: force of 130 N, wheel angular velocity of 6000 rpm, abrasion total length of 4309 m, and AFS 50-70 quartz particles.

Once the isothermal treatment was completed, 25.4 mm x 76.2 mm x 7.6 mm specimens were subjected to abrasion testing. Contacting faces were polished up to P600 sandpaper (particle size of 25.8 μm). Volume loss was the main indicator of abrasive wear, whose estimation took into account mass loss and material density (7700 kg/m³).

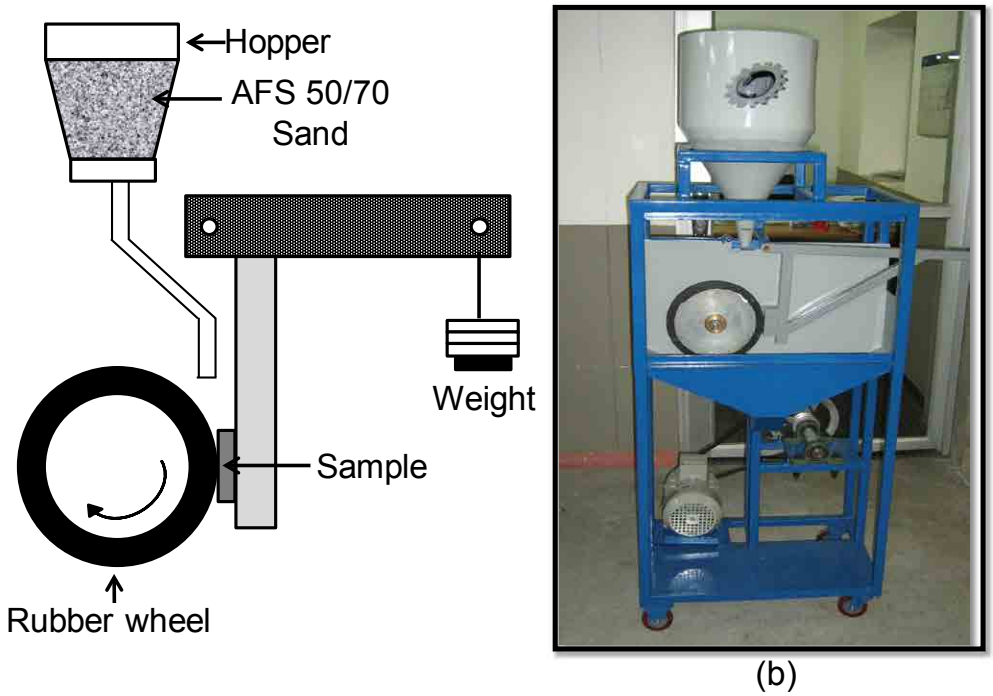

Fig. 2. (a) Scheme for a ASTM G65 three-body abrasion tester [8, 9]; (b) Actual dry sand/rubber wheel apparatus.

III. Results and analysis

A. Characterization

Fig. 3(a) depicts the microstructure of the material before isothermal treatment, which consist of eutectic austenite (γ) + chromium carbides. EDS spectrum of chemical composition (Fig. 3b) corroborates the presence of high contents of chromium and a low percentage of silicon. Additionally, as seen in Fig. 4, typical XRD spectrum of HCWCI before isothermal treatment identifies the microstructure (matrix and type of precipitates), where diffraction peaks attest to the presence of ferrite, primary austenite (proeutectic), secondary austenite (eutectic), and eutectic orthorhombic ($(Fe,Cr)_7C_3$) and cubic ($(Fe,Cr)_{23}C_6$) carbides.

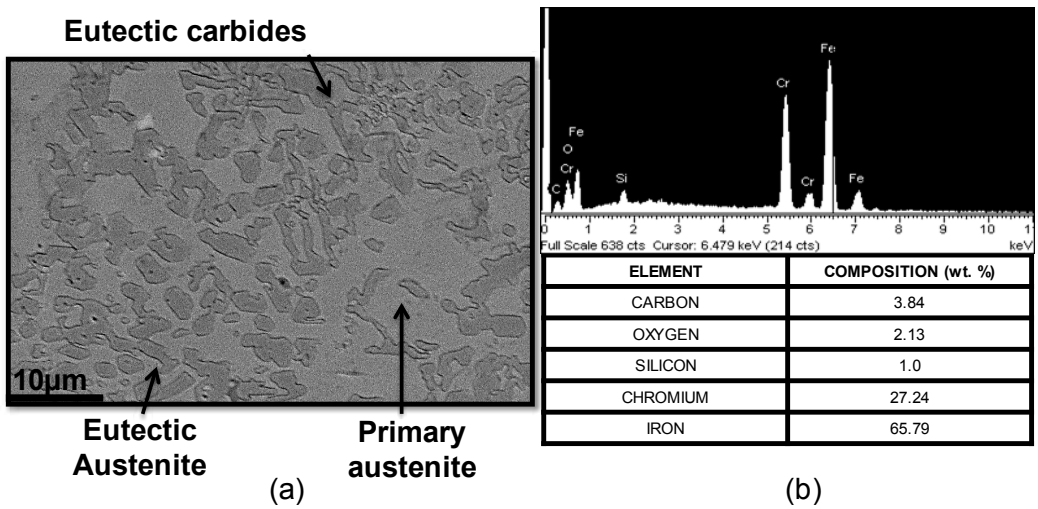

ELEMENT	COMPOSITION (wt. %)
CARBON	3.84
OXYGEN	2.13
SILICON	1.0
CHROMIUM	27.24
IRON	65.79

Fig. 3. Characterization of HCWCI before isothermal treatment (a) SEM; (b) EDS spectrum.

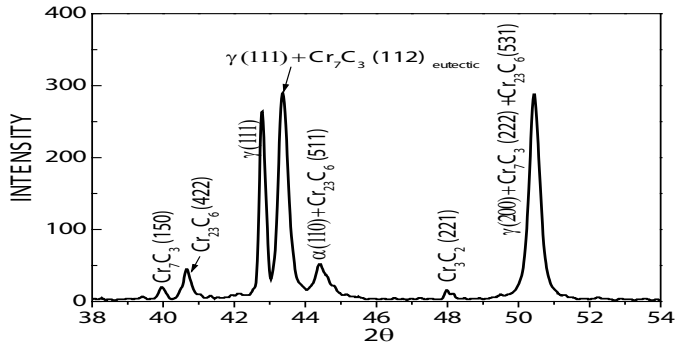

Fig. 4. XRD spectrum of HCWCI in delivery status.

XRD analysis focused on angles 2θ (Bragg angles) from 38 to -54º. For better clarity, Miller Indexes (hkl) of weaker intensities of diffraction were neglected (2 % in respect to the highest intensity) [10]. Besides the typical diffraction peaks of austenite (111), (200) and ferrite (110), Fig. 4 also verifies the presence of the eutectic carbides, Cr_7C_3 in planes (150), (112), (151), (222), and $Cr_{23}C_6$ in planes (422), (511) and (531) [10].

Fig. 5 reports the equilibrium of the HCWCI phases with fixed percentages of chromium (25 %) and Carbon (3 %). In respect to 3.02 % C at temperatures lower than 650 ºC, there is a presence of chromium carbides (K_2+ K1) in a ferritic matrix corresponding to $(Fe,Cr)_7C_3$ and $(Fe,Cr)_{23}C_6$ respectively [11, 12]. This high percentage of chromium decreased the amount of carbon (from 4.3 to 3.02 %) and increased the temperature (from 1147 ºC to 1280 ºC of the eutectic point); thereby, promoting a major presence of stable chromium carbides [6].

Due to its carbon percentage, HCWCI reports liquidus, solidus and eutectic temperatures different from those presented in the unalloyed white cast irons (1290, 1260 and 1270 ºC respectively) [13,14]. However, as the carbon content dissolves in the austenite, and the tendency of eutectoid transformation increases, these temperatures of phase transformation tend to decrease due to the reduction of austenite stability in the transformation zone (Fig. 5a). In the cases of fixed carbon (Fig. 5b), a reduction of temperatures of crystallization and eutectic transition is observed. A rise of temperature range between solid and liquid phases takes place when reducing the chromium content; that is, this range decreases with the increase of the ratio chromium/carbon, while the value is minimum at eutectic temperature [16, 17]. Chromium increase (Fig. 5b) implies narrowing of the austenite phase (γ phase), expansion of the zone $\alpha + K_1 + K_2$ and increase of the temperature of eutectic transition. The result of such eutectic transformation is given by $\gamma + M_7C_3$ [18].

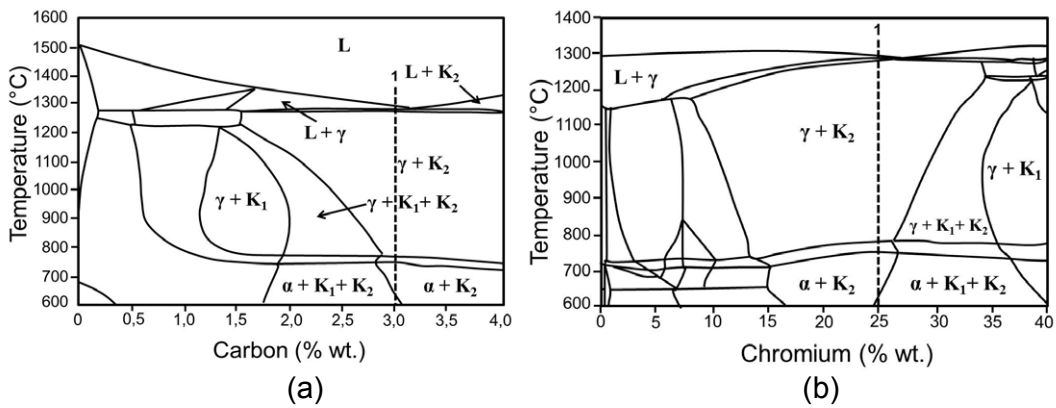

Fig. 5. Equilibrium phases of the metallic systems. (a) Fe-C 25%Cr (fixed) with C variation; (b) Fe-Cr 3%C (fixed) with Cr variation [15].

B. Wear resistance

The behavior against abrasive wear of ASTM A 532 can be seen in Fig. 6, where a significant improvement is verified for all austempering conditions in comparison to delivery-supply status. Such improvement can be explained by the formation of a variety of microstructures in terms of holding times at austempering temperatures. At the highest austempering temperature (650 °C), progressive precipitation of secondary laminar compounds, mainly $Cr_{23}C_6$ type, was observed; further, longer holding times promoted the formation of localized zones where $Cr_{23}C_6$ carbides started to transform into Cr_7C_3 type [7, 8]. Such transformation is determinant for abrasive wear resistance at 650 °C.

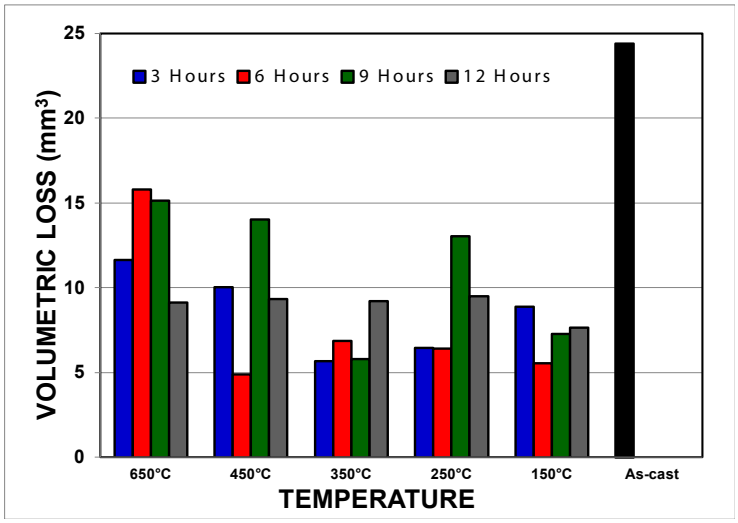

Fig. 6. Volume loss in respect to different austempering temperatures of HCWCI ASTM A 532.

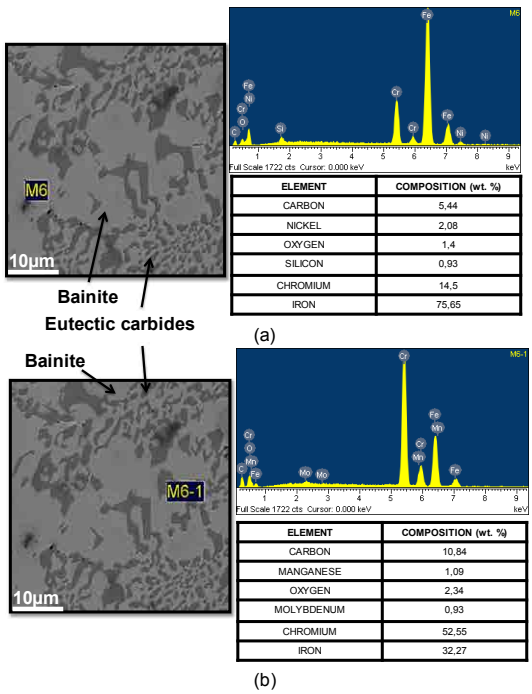

ELEMENT	COMPOSITION (wt. %)
CARBON	5,44
NICKEL	2,08
OXYGEN	1,4
SILICON	0,93
CHROMIUM	14,5
IRON	75,65

ELEMENT	COMPOSITION (wt. %)
CARBON	10,84
MANGANESE	1,09
OXYGEN	2,34
MOLYBDENUM	0,93
CHROMIUM	52,55
IRON	32,27

Fig. 7. Microstructure at austempering temperatures of 450 ºC (holding time of 6 hours). (a) Bainite Matrix (Zone M6); (b) Eutectic Carbides (Zone M6-1).

According to Fig. 6, the best wear resistance was found at austempering temperatures of 450 and 150 °C (holding time of 6 hours). Microstructures corresponding to the former case, consists of a bainite matrix (zone M6 of Fig. 7a) with high contents of carbon and chromium (ausferrite), and alloyed carbides Type I with high content of chromium produced during the solidification phase (M_7C_3 and $M_{23}C_6$); whereas during austempering at 150 °C, the main precipitated compounds are eutectic carbides with high content of chromium type II (M_7C_3), as seen in zone M6-1 of Fig. 7b. This microstructure was confirmed with XRD (Fig. 9).

At the lowest austempering temperature (150 °C), the best wear resistance was expected. However, an incomplete transformation to martensite, due to the presence of retained austenite, did not prompt the expected result. Despite this, all the austempering conditions at 150 °C yielded a wear resistance as satisfactory as those achieved at 350 °C with holding times of 3 and 9 hours. Regarding the microstructure at 350 °C, Fig. 9 shows a bainite/martensite matrix with primary eutectic carbides of chromium (M_7C_3),

and secondary Cr_7C_3, Cr_3C_2 and $Cr_{23}C_6$. Finally, less favorable results occurred after holding times of 6 hours at austempering temperatures of 650 ºC, and after holding times of 9 hours at 650, 450 and 250 ºC.

For all the austempering conditions, the following abrasive wear mechanisms were reported: ploughing, spalling, plastic deformation and formation of pits. Fig. 8 depicts traces of abrasive wear at 650 °C (holding time of 3 hours) and at 350 °C (holding time of 9 hours). Debris detachment, mostly due to cutting, can be explained by the differences of hardness between the abrasive agent (1900-2000 HV) and the obtained contacting face of the matrices: martensite (770-800 HV), bainite (600-800 HV), retained austenite (300-400 HV) or any combination of them. Retained austenite has been reported [20] as the cause of plastic deformation, ploughing and spalling of superficial layers of material.

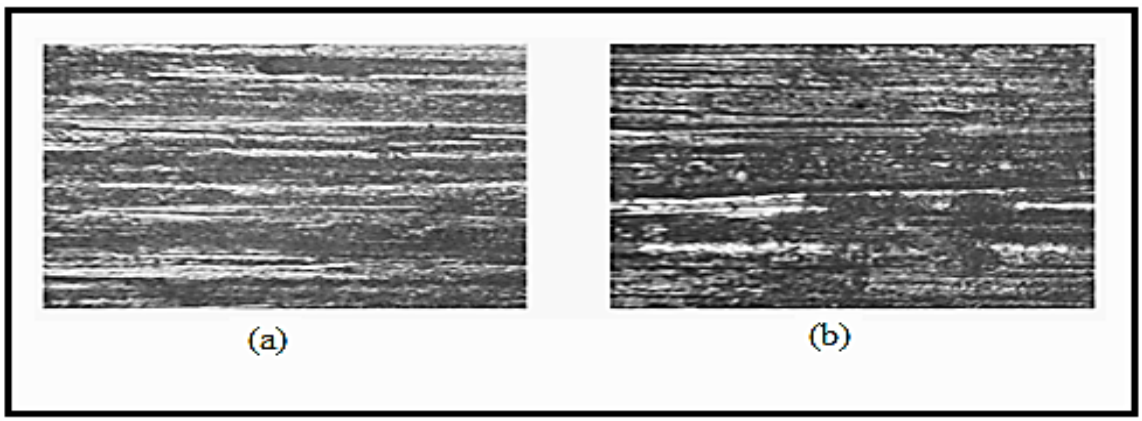

Fig. 8. Traces of abrasive wear presented in ASTM A 532. (a) 650 °C (holding time of 3 hours); (b) 350 °C (holding time of 9 hours).

The carbides obtained in this study exhibited a hardness range from 1000 to 2000 HV. Usually for all the carbides, shear stress by abrasive particles results in direct tearing of the material attested by the presence of pits [18, 19].

C. Microstructure variation during austempering

XRD peaks in Fig. 9 corroborate the presence of matrices: martensite (ά), bainite (110), and austenite (111) and (200). XRD planes also confirm the presence of carbides: Cr_7C_3 (150), (112), (151), (222), $Cr_{23}C_6$ (511), and Cr_3C_2 (230) and (221). The presence of austenite was constant for all the cases; thus, it did not undergo complete transformation. The peaks corresponding to martensite (250 and 150 °C) and bainite (650 and 350 °C) can be seen within the range 43.8-45.2° (Fig. 9); a slight displacement of them was observed, which indicates internal stress due to transformation. The most representative displacement occured at 250 °C and can be explained by the presence of a mixed matrix of martensite-bainite with little amount of retained austenite.

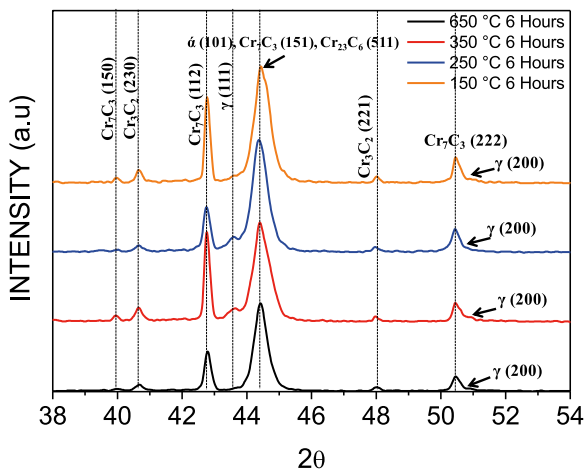

Fig. 9. XRD results for HCWCI at different austempering temperatures with holding times of 6 hours.

IV. Conclusions

Status-delivery status of HCWCI consisted of primary austenite dendrites in low proportion and a eutectic mixture of chromium carbides with eutectic austenite

(M_7C_3/austenite). It is also reported a little amount of martensite in the boundaries of carbides, due to chromium impoverishment in the matrix.

Heat treatment involving austenizing and austempering drastically modified the microstructure, leading to the precipitation of carbide particles of type $M_{23}C_6$ in the matrix. Decreasing austempering temperatures and increasing holding times resulted in a larger amount of carbides, hence a greater martensite transformation. Eutectic carbides are not affected by heat treatment; thus, the dendrite microstructure remains the same.

The least volume loss was achieved for the case of austempering at 450 ºC with holding time of 6 hours, thanks to a homogeneous mixture of bainite with high content of chromium and carbon (ausferrite), and eutectic carbides ($(Fe,Cr)_7C_3$, $(Fe,Cr)_{23}C_6$).

References

[1] M. Col, F. GülKoc, H. Öktem, and D. Kir, "The role of boron content in high alloy white cast iron (Ni-Hard 4) on microstructure, mechanical properties and wear resistance," *Wear*, vol. 348-349, pp 158-165, Feb. 2016. DOI: http://doi.org/10.1016/j.wear.2015.12.007.

[2] K. Kusumoto, K. Shimizu, X. yaer, Y. Zhang, Y. Ota, and J. Ito, "Abrasive wear characteristics of Fe-2C-5Cr-5Mo-5W-5Nb multicomponent white cast iron," *Wear*, vol. 376-377, pp 22-29, Apr. 2017. DOI: http://doi.org/10.1016/j.wear.2017.01.096.

[3] K.D Tozetti, E. Albertin, and C. Scandian, "Abrasive size and load effects on the wear of a 19.9 % chromium and 2.9 % carbon cast iron," *Wear*, vol. 376-377, pp 46-53, Apr. 2017. DOI: http://doi.org/10.1016/j.wear.2017.02.008.

[4] V. Heino, M. Kallio, K. Valtonen, and V. T. Kuokkala, "The role of microstructure in high stress abrasion of white cast irons," *Wear*, In press. Mayo 2017. DOI: http://doi.org/10.1016/j.wear.2017.04.029.

[5] American Society for Testing and Metals. Standard Specification for Abrasion Resistant Cast Irons: ASTM G-532,

[6] J. P. Holman, *Transferencia de calor*, 8 Ed. McGraw Hill, 1998.

[7] ASM Handbook, Vol. 1, *Properties and Selection: Irons, Steels, and High-Performance Alloys*, 1993.

[8] ASM Handbook, vol. 18, *Friction, Lubrication, and Wear Technology, 1992*.

[9] American Society for Testing and Metals. Standard Test Method for Measuring Abrasion Using the Dry Sand/Rubber Wheel Apparatus: ASTM G-65.

[10] S. D. Carpenter, and D. Carpenter, "X-ray diffraction study of M7C3 carbide within a high chromium white iron," *Materials Letters,* vol. 57 (28), pp. 4456-4459, Oct. 2003. DOI: http://doi.org/10.1016/S0167-577X(03)00342-2.

[11] C. Fan, M. C. Chen, C.M. Chang, and W. Wu, "Microstructure change caused by (Cr, Fe)23C6 carbides in high chromium Fe–Cr–C hardfacing alloys," *Surf. Coat. Technol*ogy, vol. 201 (3-4), pp. 908-912, Oct. 2006. DOI: http://doi.org/10.1016/j.surfcoat.2006.01.010.

[12] Ö. N. Doğan, J. A. Hawk, and G. LairdII, "Solidification Structure and Abrasion Resistance of High Chromium White Irons," *Metall. Mater. Trans. A*., vol. 28A, pp 1315-1328, Jun. 1997. DOI: http://doi.org/10.1007/s11661-997-0267-3.

[13] A. E. Karantzalis, A. Lekatou, and E. Diavat, "Effect of Destabilization. Heat Treatments on the Microstructure of High-Chromium Cast Iron: A Microscopy Examination Approach," *J. Mater. Eng. Perform.,* vol 18 (8), pp 1078-1085, Nov. 2009. DOI: http://doi.org/10.1007/s11665-009-9353-6.

[14] S. K. Hann, and J. D.Gates, "A transformation toughening white cast iron," *J. Mater. Sci.,* vol. 32 (5), pp. 1249-1259, Mar. 1997. DOI: http://doi.org/10.1023/A:1018544204267.

[15] D. Li, L. Liu, Y. Zhang, Ch. Ye, X. Ren, Y. Yang, and Q. Yang, "Phase diagram calculation of high chromium cast irons and influence of its chemical composition," *Materials and Design.,* vol. 30 (2), pp. 340-345, Feb. 2009. DOI: http://doi.org/10.1016/j.matdes.2008.04.061.

[16] A. Bedolla-Jacuide, L. Arias, and B. Hernández, "Kinetics of Secondary Carbides Precipitation in a High-Chromium White Iron," *J. Mater. Eng. Perform*, vol. 12 (4), pp. 371-382, Aug. 2003. DOI: http://doi.org/10.1361/105994903770342881.

[17] A. E. Karantzalis, A. Lekatou, and H. Mavros, "Microstructural Modifications of As-Cast High-Chromium White Iron by Heat Treatment," *J. Mater. Eng. Perform*., vol. 18 (2), pp. 174-181, Mar. 2009. DOI: http://doi.org/10.1007/s11665-008-9285-6.

[18] A. Akhbarizadeh, A. Shafyei, and M.A. Golozar, "Effects of cryogenic treatment on wear behavior of D6 tool steel," *Materials and Design,* vol. 30 (8), pp. 3259-3264, Sep. 2009. DOI: http://doi.org/10.1016/j.matdes.2008.11.016.

[19] Y. P. Wang, D. Y. Li, L. Parent, and H. Tian, "Performances of hybrid high-entropy high-Cr cast irons during sliding wear and air-jet solid-particle erosion," *Wear* 301, pp. 390-397, 2013. DOI: http://doi.org/10.1016/j.wear.2012.12.045.

[20] R. Blickensderfer, J.H. Tylczak. and G. Laird II, "Spalling of high chromium white cast in balls subjected to repetitive impact," *Wear of Metals*, vol. 1, pp. 175-183, Jan. 1989.